Navier-Stokes simulation of transonic vortex flow over a delta wing

Anand Kumar

Computational and Theoretical Fluid Dynamics Division
National Aerospace Laboratories, Bangalore 560 017, INDIA

Abstract: An explicit multi-stage Runge-Kutta time-stepping scheme with cell-centred finite volume spatial discretisation is employed to solve three-dimensional, compressible Navier-Stokes equations. A novel variation for computation of viscous fluxes is used. Convergence to steady state is expedited through acceleration techniques. The vortex flow over a 65° cropped rounded leading edge delta wing is computed, and the results are compared with experimental data and Euler solution.

1. Introduction

The flowfield over a low aspect ratio delta wing at angles of attack is characterised by the separation of flow from the leading edges and the formation of two counter rotating primary vortices over the wing. These vortices induce suction pressure over the upper surface of the wing and augment the lift that can be attained through attached flow. The flow moving outboard encounters an adverse pressure gradient induced by the primary vortices, and can separate to form secondary vortices. At some high angles of attack there is a rapid change in the structure of the vortex core and associated diminishing of the induced suction in the vortex. This is known as vortex breakdown. When vortex breakdown occurs above the wing, it affects the lift, drag and the pitching moment, and can critically affect the performance of the aircraft. Since modern high-performance aircraft configurations and other aerodynamic vehicles take advantage of the augmented lift due to the highly non-linear interacting vortices present at moderate to high angles of attack, analysis of the vortex flow on delta wings has been an area of intense research (see Newsome and Kandil 1987 for a review).

Numerical computations of vortex flow were initially done by panel methods. With the advances in computational capabilities since early 1980's, Euler solvers have been used, which show that the primary vortices on the wing are captured without the use of any additional conditions or modelling (Eriksson and Rizzi 1982, Raj and Sikora 1984, Kumar and Das 1986). An experimental and theoretical programme known as 'International Vortex Flow Experiment on Euler Code Validation' was started in 1983. Detailed experimental investigations were carried out to study vortex flow physics and to provide the much needed data for validation of computational methods. The programme proposed a 65° cropped delta wing of aspect ratio 1.38, with sharp, round or drooped leading edges, and with or without a strake. The experimental measurements and results of numerical simulation based on Euler equations were presented at a Symposium held in 1986 (Elsenaar and Eriksson 1986).

The separation from the sharp leading edge wing is fixed at the geometrical singularity, which is also the case for the Euler solution. The situation is, however, more complex for the round leading edge wing, where separation is determined by the action of viscosity in the boundary layer. Viscosity is also responsible for secondary separation, which in turn displaces the primary vortex, and the shock-boundary layer interaction. The comparison

of the Euler solution with experimental pressure presented at the symposium, was *mi* good for the round leading edge wing. It seems that a viscous model is needed to give a more realistic simulation of the flow and better comparison with the experiment.

Navier-Stokes methods have been employed to compute the vortex flow over delta wings (Fujii and Kutler 1984, Rizzetta and Shang 1986, Thomas *et al.* 1987, Müller and Rizzi 1989, Kumar 1989, Kaynak *et al.* 1990, Hilgenstock 1991). The comparison with experimental data shows that the computed solutions give a more realistic simulation of the flow,

In the present paper, a cell-centred finite-volume space discretisation scheme with explicit Runge-Kutta time-stepping scheme is developed for the solution of the Navier-Stokes equations for laminar flows. An explicit, Runge-Kutta time-stepping method was first developed for the solution of Euler equations (Jameson *et al.* 1981, Kumar 1985, Radespiel and Kroll 1985). Later, the method was extended to solve the Navier-Stokes equations (Hasse *et al.* 1984, Agrawal and Deese 1984, Swanson and Turkel 1985 among others) by a suitable evaluation of the derivative terms in the viscous part of the fluxes.

The Navier-Stokes method developed here is applied to compute the transonic vortex flow over the 65° round leading edge cropped delta wing proposed by the International Vortex Flow Experiment on Euler Code Validation (Elsenaar and Eriksson 1986), and the computed results are compared with experimental data and the Euler solution.

2. Governing equations

The unsteady, three-dimensional Navier-Stok.es equations, neglecting body forces and heat sources, can be written in nondimensional integral form as follows:

$$\frac{\partial}{\partial t}\iiint_V W dV + \iint_{\partial V} \overline{F}\cdot\vec{n}dS = 0 \tag{1}$$

where $\vec{W}$ is the vector of conserved quantities given by

$$\vec{W} = \begin{bmatrix} \rho \\ \rho u \\ \rho v \\ \rho w \\ \rho E \end{bmatrix} \tag{2}$$

ρ, $\vec{u}$, (u, v, w), p, T, E and H denote the density, velocity, Cartesian velocity components, pressure, temperature, total internal energy, and total enthalpy, respectively. The quantity V denotes an arbitrary control volume with the boundary ∂V and the outer normal n. The flux tensor F may be divided into its convective part $\overline{F}_c$ and its viscous part F_v as

$$\overline{F} = \overline{F}_c - \overline{F}_v \tag{3}$$

$$\overline{F}_c = \begin{bmatrix} \rho\vec{u} \\ \rho u\vec{u} + p\vec{i}_x \\ \rho v u + p\vec{i}_y \\ \rho w u + p\vec{i}_z \\ (\rho E + p)\vec{u} \end{bmatrix}, \quad \overline{F}_v = \begin{bmatrix} 0 \\ \overline{\tau}\cdot\vec{i}_x \\ \overline{\tau}\cdot\vec{i}_y \\ \overline{\tau}\cdot\vec{i}_z \\ \overline{\tau}\cdot\vec{u} - \vec{q} \end{bmatrix} \tag{4}$$

The components of stress tensor f are given by

$$\begin{aligned}
\tau_{xx} &= 2\mu u_x - 2/3\mu\,(u_x + v_y + w_z) \\
\tau_{yy} &= 2\mu v_y - 2/3\mu\,(u_x + v_y + w_z) \\
\tau_{zz} &= 2\mu w_z - 2/3\mu\,(u_x + v_y + w_z) \\
\tau_{xy} &= \tau_{yx} = \mu\,(u_y + v_x) \\
\tau_{xz} &= \tau_{zx} = \mu\,(u_z + w_x) \\
\tau_{yz} &= \tau_{zy} = \mu\,(v_z + w_y)
\end{aligned} \tag{5}$$

and the components of heat-flux vector q are given by

$$q_x = -kT_x, \quad q_y = -kT_y, \quad q_z = -kT_z \tag{6}$$

The viscosity, μ, is assumed to follow an empirical power law

$$\mu = \left(\gamma^{1/2} M_\infty / Re_\infty\right)(T/T_\infty)^{0.75} \tag{7}$$

and the thermal conductivity, k, is given by

$$k = \frac{\gamma}{\gamma - 1}\mu / Pr \tag{8}$$

where M_∞ is the free-stream Mach number, Re_∞ is the free-stream Reynolds number, Pr is Prandtl number and 7 is the ratio of specific heats. The pressure and temperature are given by

$$p = (\gamma - 1)\,\rho\,(E - \vec{u}\cdot\vec{u}/2) \tag{9}$$

$$T = p/\rho \tag{10}$$

8, Spatial Discretisation

The discretisation of Eq, (1) follows the method of lines, i.e., discretisations in space and time are done separately. The computational domain is divided into hexahedral cells. The variables, located at cell centres, can be considered to be the average value within a cell, i.e.,

$$\vec{W}_{i,j,k} = \frac{1}{V_{i,j,k}} \int_{V_{i,j,k}} \vec{W}\,dV \tag{11}$$

where the subscript i,j,k refers to the values for the cell i,j,k. Integration of Eq. (1) over the cell i,j,k, is approximated by the discrete form of the equation

$$\frac{d}{dt}\vec{W}_{i,j,k} \quad \begin{matrix} 1 \\ V_{i,j,k} \end{matrix} \quad \begin{matrix} \cdot \\ i,j,k \end{matrix} \quad \begin{matrix} \\ i,j,k \end{matrix} \tag{12}$$

where $\vec{Q}_c$ and $\vec{Q}_v$ are the net convective and viscous flux vectors, respectively.

$\vec{Q}_c$ is obtained by integration of F_c over the six faces of the hexahedron, and similarly $\vec{Q}_v$ by integration of $-\overline{F}_v$. Thus, Q_c is given by

$$\begin{aligned}
\vec{Q}_{c_{i,j,k}} = {} & \overline{F}_{c_{i+1/2,j,k}} \cdot \vec{S}_{i+1/2,j,k} - \overline{F}_{c_{i-1/2,j,k}} \cdot \vec{S}_{i-1/2,j,k} \\
& + \overline{F}_{c_{i,j+1/2,k}} \cdot \vec{S}_{i,j+1/2,k} - \overline{F}_{c_{i,j-1/2,k}} \cdot \vec{S}_{i,j-1/2,k} \\
& + \overline{F}_{c_{i,j,k+1/2}} \cdot \vec{S}_{i,j,k+1/2} - \overline{F}_{c_{i,j,k-1/2}} \cdot \vec{S}_{i,j,k-1/2}
\end{aligned} \tag{13}$$

where, *e.g.*, $\overline{F}_{c_{i+1/2,j,k}}$ is the value of F_c on the face between the cells i, j, k and $i+1, j, k$ whose surface vector is $S_{i+1/2,j,k}$. $\overline{F}_{c_{i+1/2,j,k}}$ is evaluated by

$$\overline{F}_{c_{i+1/2,j,k}} = \overline{F}_c \left(1/2 \left(W_{i,j,k} + W_{i+1,j,k}\right)\right) \tag{14}$$

Evaluation of the viscous flux tensor $\overline{F}_v$ requires computation of first derivatives of the flow variables. One way of computing the first derivatives is to use the gradient theorem

$$\nabla\phi = \frac{1}{V}\int_{\partial V} \phi \vec{n} dS \tag{15}$$

where $\phi = u, v, w$ or T. In the present work the first derivatives are computed from the relation

$$\phi_x = \phi_\xi \xi_x + \phi_\eta \eta_x + \phi_\zeta \zeta_x \tag{16}$$

The metric terms, ξ_x, *etc.*, of the transformation from the Cartesian coordinates x, y, z to the curvilinear coordinates ξ, η, ζ are computed from

$$\nabla\xi = \vec{S}_\xi / V\,, \quad \nabla\eta = S_\eta / V\,, \quad \nabla\zeta = S_\zeta / V \tag{17}$$

where S_ξ, S_η and $\vec{S}_\zeta$ are the surface area vectors of the cell faces (Fletcher 1991). The derivatives, ϕ_ξ, *etc.*, in Eq. (16) are approximated using central differences. The derivative terms in the stress tensor and in the heat flux vector are evaluated at the cell comers, which are then averaged to give values at the cell faces, *e.g.*,

$$\phi_{x_{i+1/2,j,k}} = 1/4 \left(\phi_{x_{i+1/2,j+1/2,k+1/2}} + \phi_{x_{i+1/2,j-1/2,k+1/2}} + \phi_{x_{i+1/2,j+1/2,k-1/2}} + \phi_{x_{i+1/2,j-1/2,k-1/2}}\right) \tag{18}$$

The present scheme of evaluating the first derivatives is equivalent to spatial discretisation of the viscous flux tensor using 27 points as opposed to the conventional 19 points (see, *e.g.*, Swanson and Turkel 1985) if the gradient theorem, Eq. (15), is used at the centre of cell-faces. Müller and Rizzi (1989) use the gradient theorem to compute the derivatives at the cell centres, which are then averaged to obtain the values on the cell faces. This leads to a 25-point stencil for the spatial discretisation of the viscous flux tensor. The stencil however extends to two cells on either side and would require careful treatment at the boundary. Let this scheme be designated as Scheme A.

An alternate scheme can be constructed where the derivative terms using the local coordinate transformation are directly evaluated at the cell faces. Let this scheme be designated as Scheme B. Thus, Scheme A has a 27-point stencil as opposed to 19-point stencil of scheme B. Scheme A gives a symmetric formula, which is not the case for Scheme B. Further, Scheme A requires N evaluations compared to $3N$ evaluations for Scheme B, where N is the number of cells. Thus, the difference between operation count for the full Navier-Stokes equations and for the thin-layer Navier-Stokes equations is only marginal for Scheme A. For the thin-layer Navier-Stokes equations Scheme B would become competitive with Scheme A.

4. Artificial Dissipation

The spatial discretisation of the flux terms considered in Section 3 is equivalent to central differencing and does not damp unphysical oscillations. The finite-volume scheme is intrinsically dissipative in the regions, such as boundary layers and wake regions, where viscous terms dominate. Away from these regions the flow becomes convection dominated

and also viscous terms are poorly resolved, which may lead to undamped oscillations common to Euler equations. Therefore, artificial dissipation terms are needed to suppress any "odd-even decoupling" and to prevent oscillations in the vicinity of shock waves. On addition of artificial dissipation, Eq. (12) is replaced by

$$\frac{d}{dt}\vec{W}_{i,j,k} = \frac{1}{V_{i,j,k}}\left[\vec{Q}_{c_{i,j,k}} + \vec{Q}_{v_{i,j,k}} - \vec{D}_{i,j,k}\right] \tag{19}$$

where $D_{i,j}k$ is the artificialdissipation term. The artificial dissipation model of Jameson *et al.* (1981) is adopted here. The model consists of a blend of second and fourth differences with coefficients depending on the local pressure graient. The artificial dissipation term is constructed as

$$\vec{D}_{i,j,k} = d_{i+1/2,j,k} - d_{i-1/2,j,k} + d_{i,j+1/2,k} - d_{i,j-1/2,k} + d_{i,j,k+1/2} - d_{i,j,k-1/2} \tag{20}$$

The terms on the right hand side have a similar form.

$$d_{i+1/2,j,k} = \bar{\lambda}_{\xi_{i+1/2,j,k}}\left[\epsilon^{(2)}_{i+1/2,j,k}\Delta_\xi - \epsilon^{(4)}_{i+1/2,j,k}\Delta_\xi\nabla_\xi\Delta_\xi\right]\vec{W}_{i,j,k} \tag{21}$$

where Δ_ξ, and ∇_ξ are respectively, the forward and backward difference operators in the ξ direction. A variable scaling factor, $\bar{\lambda}_{\xi_{i+1/2,j,k}}$ is employed to account for varying cell aspect ratio (Martinelli 1987, Radespiel 1989). It is a function of the spectral radii of the Jacobian matrices in the ξ, η, ζ directions,

$$\bar{\lambda}_{\xi_{i+1/2,j,k}} = \lambda_{\xi_{i+1/2,j,k}} \Phi_{i+1/2,j,k} \tag{22}$$

$$\lambda_{\xi_{i+1/2,j,k}} = \left|\vec{S}_{\xi_{i+1/2,j,k}}\right| + a\left|\vec{S}_{\xi_{i+1/2,j,k}}\right| \tag{23}$$

$$\Phi_{i+1/2,j,k} = 1 + \max\left\{\left(\lambda_{\eta_{i+1/2,j,k}}/\lambda_{\xi_{i+1/2,j,k}}\right)^\omega, \left(\lambda_{\zeta_{i+1/2,j,k}}/\lambda_{\xi_{i+1/2,j,k}}\right)^\omega\right\} \tag{24}$$

where a is the speed of sound. The value of $\omega = 0.5$ has been chosen in the present study. The coefficients $\epsilon^{(2)}$ and $\epsilon^{(4)}$ in Eq. (21) are designed to provide enough dissipation. $\epsilon^{(4)}$ controls the background dissipation and is switched off near shocks as it can have a destabilising effect on the numerical calculation. Pressure is used as sensor to locate shocks in the flow. They are defined by

$$\epsilon^{(2)}_{i+1/2,j,k} = k^{(2)} \max\left(\nu_{i-1,j,k}, \nu_{i,j,k}, \nu_{i+1,j,k}, \nu_{i+2,j,k}\right) \tag{25}$$

$$\nu_{i,j,k} = \left|\frac{p_{i-1,j,k} - 2p_{i,j,k} + p_{i+1,j,k}}{p_{i-1,j,k} + 2p_{i,j,k} + p_{i+1,j,k}}\right| \tag{26}$$

$$\epsilon^{(4)}_{i+1/2,j,k} = \max\left[0, \left(k^{(4)} - \epsilon^{(2)}_{i+1/2,j,k}\right)\right] \tag{27}$$

In the dissipation term in the energy equations ρH is used insted of pE so that constant H can be a solution of the energy equation.

The dissipation terms are of third order in smooth regions of the flow and become of order one in the neighbourhood of the shocks.

5. Time Stepping Scheme

A modified, five-stage Runge-Kutta scheme is used for the time integration of the system of ordinary differentia! equations obtained by spatial discretisation. At the time level n the solution is advanced

$$\begin{aligned} &\vec{W}^{(0)} = \vec{W}^n \\ &\vec{W}^{(m+1)} = \vec{W}^{(0)} - \alpha_{m+1}\Delta t R^{(m)}, \quad m = 0, 1, \ldots, 4 \\ &\vec{W}^{n+1} = \vec{W}^{(5)} \end{aligned} \tag{28}$$

where Δt is the time step. The residual $R^{(m)}$ is given by

$$R^{(m)} = \frac{1}{\vec{V}}\left(\vec{Q}_c^{(m)} + \vec{Q}_v^{(0)} - \sum_{n=0}^{m} \gamma_{mn}\vec{D}^{(n)}\right) \tag{29}$$

where $\vec{Q}_c^{(m)} = Q_c\left(\vec{W}^{(m)}\right)$, $\vec{Q}_v^{(0)} = Q_v\left(\vec{W}^{(0)}\right)$, and $\vec{D}^{(m)} = D\left(\vec{W}^{(m)}\right)$. The viscous fluxes, $\vec{Q}_v$, are computed in the first stage and kept frozen for the remaining stages. The artificial dissipation terms are computed in the first, third and fifth stages of the algorithm. The coefficients α_m are

$$\alpha_1 = 1/4, \ \alpha_2 = 1/6, \ \alpha_3 = 3/8, \ \alpha_4 = 1/2, \ \alpha_5 = 1 \tag{30}$$

The weighting factors of the artificial dissipation satisfy the consistency condition,

$$\sum_{n=0}^{m} \gamma_{mn} = 1 \tag{31}$$

and are

$$\begin{gathered} \gamma_{00} = 1, \\ \gamma_{10} = 1, \quad \gamma_{11} = 0, \\ \gamma_{20} = (1 - \bar{\gamma}_3), \quad \gamma_{21} = 0, \quad 722 = \gamma_3, \\ 730 = (1 - \bar{\gamma}_3), \quad 731 = 0, \quad \gamma_{32} = \gamma_3, \quad 733 = 0, \\ 740 = (1 - \bar{\gamma}_3)(1 - \bar{\gamma}_5), \quad \gamma_{41} = 0, \quad \gamma_{42} = \gamma_3(1 - \bar{\gamma}_5), \quad \gamma_{43} = 0, \quad 744 = \gamma_5 \\ \gamma_3 = 0{,}56, \quad \gamma_5 = 0.44 \end{gathered} \tag{32}$$

The modified Runge-Kutta scheme, Eq. (28), requires less storage than compared to the classical Runge-Kutta scheme. The Runge-Kutta schemes has the property that if $R^{(0)} = 0$ then $\bar{W}^{n+1} = \bar{W}^n$; hence, the steady state is independent of the time step. The scheme is also amenable to variety of convergence acceleration techniques.

6. Acceleration Techniques

Techniques to accelerate the convergence of the basic time stepping scheme can be employed, if the steady state solution is only of interest. The techniques employed here are as follows: (a) local time stepping, (b) implicit residual smoothing, and (c) enthalpy dampling.

With local time stepping, the solution is advanced at each mesh point by the maximum allowable time step dictated by stability. Both convection and diffusion are included in the computation of Δt,

$$A^* = CFL\left[(\lambda_\xi + \lambda_\eta + \lambda_\zeta)\, IV + c_{diff}\nu_{diff}\left(\vec{S}_\xi \cdot \vec{S}_\xi + \vec{S}_\eta \cdot \vec{S}_\eta + \vec{S}_\zeta \cdot \vec{S}_\zeta\right)/V^2\right]^{-1} \tag{33}$$

where $\nu_{diff} = \max(4/3, \gamma/Pr)\,\mu/\rho$ and $c_{diff} = 2$.

The stability of the basic Runge-Kutta time stepping scheme can be extended using implicit smoothing of the residuals (Jameson 1983). Residual averaging is applied in the form

$$(1 - \epsilon_\xi \nabla_\xi \Delta_\xi)(1 - \epsilon_\eta \nabla_\eta \Delta_\eta)(1 - \epsilon_\zeta \nabla_\zeta \Delta_\zeta)\bar{R}^{(m)} = R^{(m)} \qquad (34)$$

where $R^{(m)}$ is the explicit residual at stage m of the Runge-Kutta scheme, Eq. (28), and $\bar{R}^{(m)}$ is the residual at stage m after the smoothing in the ξ, η and ζ directions. The residual averaging is carried out at the first, third and fifth stages of the present scheme.

Enthalpy damping was introduced by Jameson *et al.* (1981) for Euler equations. Under certain assumptions the total enthalpy, H, may be taken as constant for viscous flows. In the transient phase, the difference between PI and H_∞ can be used to accelerate convergence. This is implemented by an additional damping step,

$$\vec{W}^{n+1} = \frac{1}{1 + \sigma(H^{(5)} - H_\infty)}\vec{W}^{(5)} \qquad (35)$$

with the exception that the damping step for the energy equation is

$$(\rho E)^{n+1} = \frac{1}{1+\sigma}\left((\rho E)^{(5)} - \sigma p^{(5)}\right) \qquad (36)$$

where σ is the enthalpy damping parameter.

7. Boundary conditions

The boundary condition on the wing surface is that of no-slip, and the wing surface is assumed to be adiabatic. The pressure on the wing surface is obtained by taking its normal derivative to be zero. Thus on the wing surface

$$u = v = w = 0, \quad \left.\frac{\partial T}{\partial n}\right|_w = 0, \quad \left.\frac{dp}{\partial n}\right|_w = 0 \qquad (37)$$

The inflow/outflow condition on the farfield boundary is based on Riemann invariants of one dimensional inviscid flow along the normal direction (Jameson and Baker 1983), in order that the outgoing waves are not reflected back into the flowfield. The Riemann invariants of one-dimensional inviscid flow are

$$R^- = q_n - 2a/(\gamma - 1), \quad R^+ = q_n + 2a/(\gamma - 1) \qquad (38)$$

where $q_n = u \cdot n$ is the velocity along the outer normal. The Riemann invariants $R^\pm$ are constant along the characteristics $C^\pm$: $dn/dt = q_n \pm a$, where a is the speed of sound and n is distance along the outer normal. At the end of each time step the characteristic variables corresponding to the outgoing characteristics are extrapolated from the interior, and the characteristic variables corresponding to the incoming characteristics are obtained from the freestream values. For example, for a subsonic inflow/outflow boundary, the boundary condition is implemented as follows

$$R^- = R^-_\infty = q_{n_\infty} - 2a_\infty/(\gamma - 1), \quad R^+ = R^+_e = q_{n_e} + 2a_e/(\gamma - 1) \qquad (39)$$

which gives

$$q_n = \frac{1}{2}\left(R^+_e + R^-_\infty\right), \quad a = \frac{\gamma - 1}{4}\left(R^+_e - R^-_\infty\right)$$

In the above the subscript e refers to values from interior. In addition, the tangential velocities and entropy are extrapolated from their freestream values at the inflow boundary and from their interior values at the outflow boundary.

8. Results

The round leading edge delta wing, proposed for the International Vortex Flow Experiment on Euler Code Validation, is a cropped wing having 65° sweep and 15% taper. Tk wing-section is a modified NACA 64A005 profile with nose radius of 0.7% and maximum thickness of 5% at 40% chord. The wing section normalised by local chord is given by

$$y = \begin{cases} \pm (0.1183\sqrt{x} - 0.2101x + 0.3501x^2 - 0.3406x^3) & \text{for } 0 < x < 0.4 \\ \text{NACA } 64A005 & \text{for } 0.4 \leq x \leq 1 \end{cases} \quad (40)$$

A C-O mesh around the wing is generated using the transfinite interpolation method (Eriksson 1982, Kumar 1987). The mesh consists of 97 x 33 x 33 grid points, *i.e.*, there are 97 points around the chordwise $I-$direction, 33 points along the near normal $J-$direction and 33 points along the spanwise $K-$direction. Of the 97 points in the $I-$direction, 73 points are on the wing surface. Figure 1 shows the grid on the wing surface, where the clustering of the grid near the leading edge, tip and near the trailing edge is seen. The grid in the root plane and an enlargement of it showing clustering near the wing surface, are presented in Fig. 2

Flow computations are carried out at M_∞ = 0.85, a = 10.0°, and Re_∞ (based OB root chord) = 2.38 X 10^6. The computation is first carried out on a coarse mesh of size 49 x 17 x 17 (obtained by deleting alternate lines in the final grid). The coarse mesh solution is interpolated to give the starting solution on the final mesh.

Figure 3 shows the C_p distribution at chordwise stations, $x = 0.3$, 0.6 and 0.8, along with the experimental measurements (Hartmann 1986). The origin of the coordinate system is located at the wing apex, and the x, y and z axes are along the root chord, along the normal to root chord in the root plane, and along the spanwise directions, respectively. *s(x)* in Fig. 3 is the local semispan. The positions of the suction peaks show that the predicted location of the primary vortex is in good agreement with tk experiment. The magnitude of the suction peak, however, is lower than that observed, This can be attributed to the comparatively coarse mesh used or to the non-inclusion of turbulence in the present analysis. The realism of the prediction, in comparison to the Euler method whose results (Kumar and Das 1986) show (Fig. 3) that the suction peak is far too strong and lies very close to the leading edge, is significant.

Figure 4 shows the cross flow velocity vector on an $I-$grid plane which lies close to x = 0.8 at the root chord (note that $I-$grid planes are not x = constant plane). The primary and secondary vortices are seen from the crossflow velocity vector plot. Figure 5 shows the surface streamline where reattachment of the primary vortex, secondary separation and another reattachrnent line (possibly tertiary reattachrnent) occur. The computed surface streamline can be compared to the experimental surface oil flow on a sharp leading edge wing (Bannick and Houtmann 1986), to find if the predicted position of primary reattachment and secondary separation are reasonable. This is indeed so; this comparison however is not shown here. The surface streamline also show that the secondary vortex does not start from the apex, it is seen to form at about x SB 0.3.

9. Conclusion

A Navier-Stokes method for laminar compressible flow is developed. A novel finite volume cell centred scheme for spatial discretisation of the viscous fluxes is employed which has a 27-point stencil consisting of all immediate cells. Explicit Runge-Kutta method is used for time-stepping. The method incorporates local time stepping, implicit residual averaging and enthalpy damping to accelarate the convergence to steady state. The code also has

a multi-block feature (see Kumar 1988). The method is employed to compute transonic flow over a 65° round leading edge cropped delta wing on a C-O mesh of 97 x 33 x 33 grid points. The computed solution for M_∞ = 0.85, a - 10.0° and Re_{∞,c_R} = 2.38 x 10^6 show that the location of primary vortex is well predicted. The computed flow also shows a secondary vortex that starts from about 30% of the root chord.

This is the first result from the present code. More validation is needed. Inclusion of a turbulence model is also planned. The present computation is carried out on the Magnum R3000 computer at CTFD Division, NAL. It is planned to use Flosolver, a parallel computer developed by NAL, to expedite the development and validation.

References

Agrawal, R.K. and Deese, J.E. (1984), "Computation of transonic viscous airfoil inlet and wing flowfields," AIAA Paper No. 84-1551.

Bannink, W.J. and Houtman, E.M. (1986), "Experiments on the transonic flow at high angles of attack," Proc. *International Vortex Flow Experiment on Euler Code Validation*, FFA TN, Stockholm, pp. 37-46.

Elsenaar, A. and Eriksson, G. (Eds.) (1986), Proc. *Symp. on Intl. Vortex* Flow *Experiment on Euler Code Validation*, FFA, Bromma.

Eriksson, L.E. (1982), "Generation of body conforming grids around wing-body configurations using transfinite interpolation," *AIAA* J., 20, 1313-1320.

Eriksson, L.E. and Rizzi, A. (1982), "Computation of vortex flow around wings using the Euler equations," *Proc. 4th GAMM Conf. on Num. Meth. in Fluid Mech.*, *Notes on Numerical Fluid Mechanics* H.Viviand (ed.), Vieweg, Braunschweig.

Fletcher, C.A.J, (1991), *Computational techniques for fluid dynamics - Vol. //*, Second edition, pp.51, Springer-Verlag, Berlin.

Fujii, K. and Kutler, P. (1984), "Numerical simulation of vortical flows over a strake delta wings," AIAA Paper No. 84-1550.

Hartmann, K. (1986), "US/European transonic vortex flow experiment - data lists of pressure measurements," DFVLR IB 222 - 86 A 26.

Hasse, W., Wagner, B., and Jameson, A. (1984), "Development of a Navier-Stokes method based on a finite volume technique for the unsteady Euler equations," *Proc. 5th GAMM Conf. on Num. Meth. in Fluid Mech.*, *Notes on Numerical Fluid Mechanics* M.Pandolfi and R.Piva (eds.), Vieweg, Braunschweig.

Hilgenstock, A. (1991), "Validation of transonic turbulent flows past delta wing configurations," *Aero. J.*, pp.219–230.

Jameson, A. (1983), "The evolution of computational methods in aerodynamics," *J. Appl. Mech.*, bf 50.

Jameson, A. and Baker, T.J. (1983), "Solution of Euler equations for complex configurations," AIAA Paper No. 83-1-929.

Jameson, A., Schmidt, W., and Turkel, E. (1981), "Numerical solutions of the Euler equations by finite volume method using Runge-Kutta time-stepping scheme," AIAA Paper No. 81-1259.

Kaynak, U., Tu, E., Dindar, M., and Barlas, R. (1990), 'Nonequilibrium turbulence modelling effects on transonic vortex flows about delta wings," AGARD-FDP Vortex Flow Aerodynamics.

Kumar, A. (1985), "Solution of Euler equations for transonic flow past an airfoil," NAL FM TM-8503.

Kumar, A. (1988), "Euler solutions with a multi-block structured code," *J. Aero. Soc. India*, **40**, 89–95.

Kumar, A. and Das, A. (1986), "Numerical solutions of flow fields around delta wings using Euler equations," Proc. *International Vortex Flow Experiment on Euler Code Validation* FFA TN, Stockholm, pp. 175-186.

Kumar, A. (1987), "Application of transfinite interpolation to grid Generation," *Proc. III National Conference on Aerodynamics*, IIT, Bombay.

Kumar, A. (1989), "Flow calculation over a a delta wing using the thin-layer Navier-Stokes equations," Proc. *3rd Intl. Symp. on CFD*, Nagoya, pp.371–376.

Martinelli, L. (1987), *Calculation of viscous flows with a multigrid method*, Ph.D. Dissertation, MAE Department, Princeton Univ.

Müller, B. and Rizzi, A. (1989), "Navier-Stokes computation of transonic vortices over a round leading-edge delta wing," *Intl. J. Num. Methods in Fluids*, 9, 943-962.

Newsome, R.W. and Kandil, O.A. (1987), "Vortical flow aerodynamics - physical aspect and numerical simulation," AIAA Paper No. 87-0205.

Radespiel, R. (1989), "A cell vertex multigrid method for the Navier-Stokes equations," NASA TM-101557.

Radespiel, R. and Kroll, N. (1985), "Progress in the development of an efficient finite volume code for the three-dimensional Euler equations," DFVLR-FB 85-31, DFVLR-EA, Braunschweig.

Raj, P. and Sikora, J.S. (1984), "Free vortex flows; Recent encounters with an Euler code," AIAA Paper No. 84-2142.

Rizzetta, D.P. and Shang, J.S. (1986), "Numerical simulation of leading edge vortex flow," *AIAA J.*, 24, 237-245.

Swanson, R.C. and Turkel, E. (1985), "A multistage time-stepping scheme for the Navier-Stokes equations," AIAA Paper No. 85-0035.

Thomas, J.L., Taylor, S.L., and Anderson, W.K. (1987), "Navier-Stokes computations of vortical flows over low aspect ratio wings," AIAA Paper No. 87-0207.

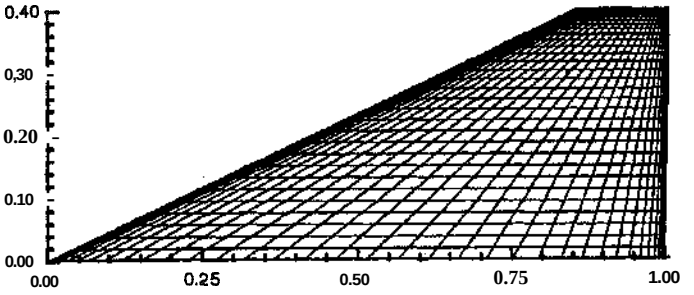

Figure 1. Grid on the wing surface

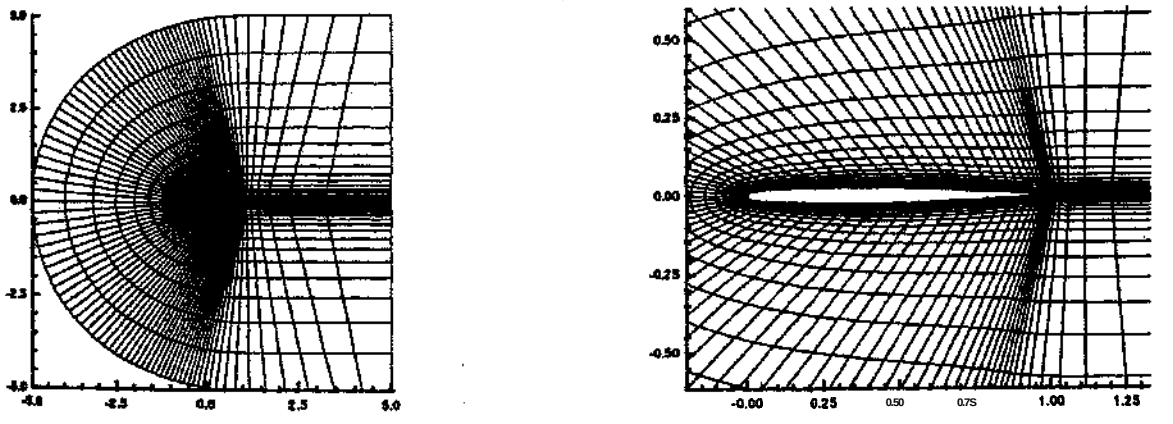

Figure 2, Root plane grid and its enlargement

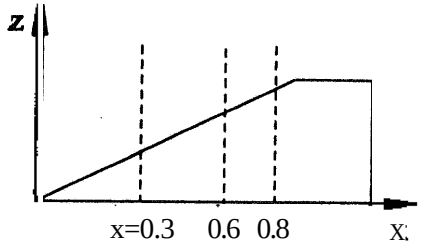

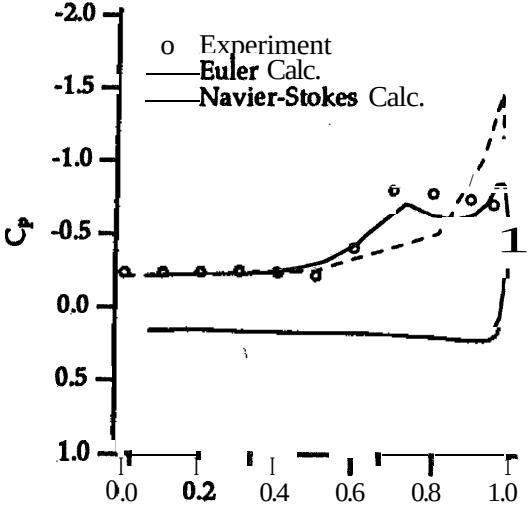

(a) x = 0.3

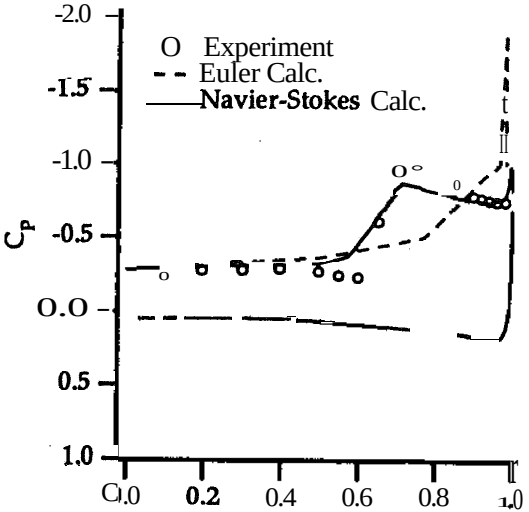

(b) x = 0.6

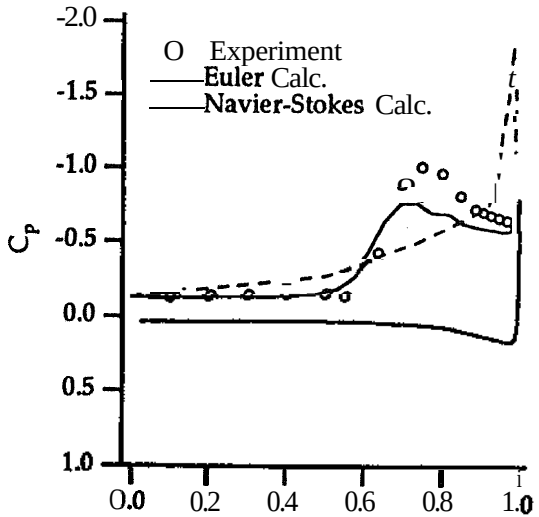

(c) x = 0.8

Figure 3. Spanwise surface pressure distributions, at three streamwise locations, for a 65° cropped delta wing with rounded leading edge. (M_∞ = 0.85, α - 10°, Re = 2.38 x 10^6)

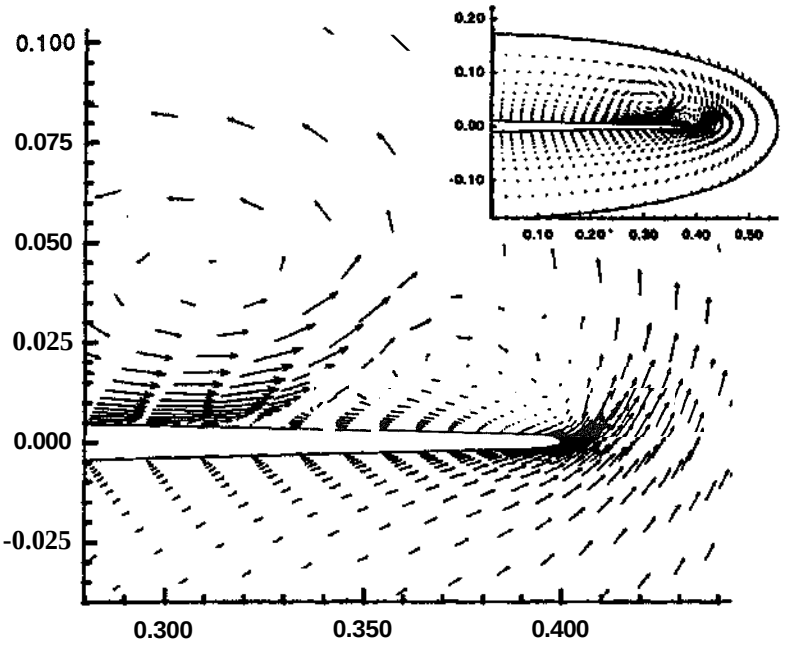

Figure 4. Cross flow velocity vectors

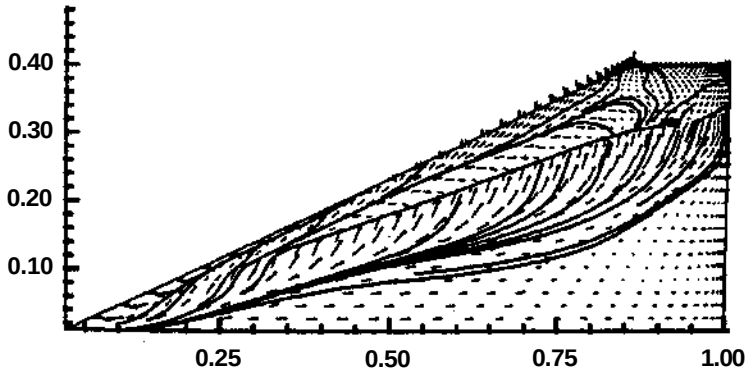

Figure 5. Surface streamlines